Catal Lett (2012) 142:541–546
DOI 10.1007/s10562-012-0811-7

Improved Thermal Stability of Pt/Al_2O_3 Cryogels by Controlling Sol–Gel Conditions

Toshihiko Osaki · Saori Shima · Takeshi Miki · Yutaka Tai

Received: 6 January 2012 / Accepted: 13 March 2012 / Published online: 31 March 2012
© Springer Science+Business Media, LLC 2012

Abstract In order to improve thermal stability and catalytic oxidation activity of platinum–alumina cryogels prepared by one-pot sol–gel reactions and subsequent freeze drying, molar ratio of aluminum sec-butoxide, nitric acid, and water used for the sol–gel processing was optimized. It was found that the sintering of platinum at high temperatures was more remarkably suppressed at $ASB:HNO_3:H_2O = 1:0.17:87$, at the ratio of which higher CO oxidation activity was also observed. It was suggested that the suppression of sintering of the metal was attributed to smaller sizes of mesopores obtained at this ratio, retarding transfer and aggregation of platinum.

Keywords Cryogel · Sol–gel · Freeze drying · Pt · Al_2O_3 · Thermal stability · Dispersion · CO oxidation · BET · XRD · TEM

1 Introduction

Platinum is one of the main components of catalysts for automotive emission gas purification; recently it has principally been used for diesel automobiles including trucks and buses. In South Africa known as one of the major precious metals producer in the world, the platinum produce cost has been increasing due to the increase of electricity cost whereas the deterioration of quality level of minerals [1]. With more people are concerned about environmental problems, automobiles companies have to address severe environmental regulations legislated by the governments of Japan, EU and the US to reduce the emission of harmful gases, which might result in increase of platinum usages. Due to the increasing production cost and the remarkable growth of demand for platinum, it has been necessary to develop high performance catalysts which contain platinum as small amount as possible. To develop such platinum-saved catalysts, it is important to improve thermal stability, this is because the metal is generally loaded in large excess in anticipation of catalyst deactivation after a long period of driving time. Previously we have synthesized thermally stable platinum–alumina cryogels by one-pot sol–gel processing and subsequent freeze drying [2, 3]. Platinum was finely distributed and stabilized throughout alumina gel support with high dispersion by the sol–gel reaction, whereas transfer and aggregation of platinum was successfully suppressed by the freeze drying, bringing about superior stability at elevated temperatures. The thermal stability might furthermore be improved by modifying fine structures of the cryogels, which may be attained by controlling sol–gel conditions [4–8]. In the present paper, molar ratio of aluminum alkoxide, nitric acid and water in one-pot sol–gel reaction was optimized to obtain preferable fine structures and textures of the cryogel enhancing the thermal stability and catalytic oxidation activity.

2 Experimental

Platinum–alumina cryogels containing 1 wt% platinum were prepared as follows. Ca. 0.029 mol of aluminum sec-butoxide (Kanto Chemicals, abbreviated hereafter as ASB) was hydrolyzed at 86 °C in ultra-pure water purified by a Milli-Q water purifier (A-10). Then 1 mol L^{-1} of nitric

T. Osaki (✉) · S. Shima · T. Miki · Y. Tai
National Institute of Advanced Industrial Science and Technology (AIST), 2266-98, Anagahora, Shimoshidami, Moriyama-ku, Nagoya 463-8560, Japan
e-mail: t-osaki@aist.go.jp

acid (Wako Pure Chemicals) was added to the sol for peptization at this temperature, stirring the sol for 1 h [9]. Molar ratio of nitric acid to ASB was varied in the range of 0.14–0.45 with keeping H_2O/ASB ratio of 70, whereas that of water to ASB was changed in the range of 29–126 with maintaining HNO_3/ASB ratio of 0.17. As a platinum source, an aqueous solution of H_2PtCl_6 (ca. 2.0 wt%, Tanaka Precious Metals) was used. An aqueous solution (5.1 mL) containing oxalic acid (5.2×10^{-2} mmol) and ammonia (7.4 mmol) was added little by little to the H_2PtCl_6 solution (0.74 g) at 86 °C, and the mixed solution was allowed to stand for 30 min at this temperature. Then this platinum solution was introduced to the peptized boehmite sol, stirring at 86 °C for more than 1 h. For gelation 0.2 g of urea (Wako Pure Chemicals) was added to the mixed sol; this sol was kept at 86 °C for one night without stirring. The co-gel obtained was dried in a freeze dryer (Tokyo Rikakikai, FDU-810; condenser temperature, −80 °C) under vacuum less than 10 Pa using a vacuum pump (Ulvac, GCD-051X). The dried gel was heated in air at 800 °C for 5 h. For reference, 1 wt% Pt/Al_2O_3 catalyst was prepared by a conventional impregnation technique using the same H_2PtCl_6 aqueous solution as a platinum source and commercial alumina (Taimei Chemicals, surface area: 200 $m^2\ g^{-1}$) as a support.

BET surface area, pore volume, and mean pore radius of the cryogels were measured by a volumetric N_2 gas adsorption measurement (Nippon BEL, Belsorp-mini) at a liquid nitrogen temperature. A pore radius distribution curve was calculated from an adsorption branch using the BJH (Barrett-Joyner-Halenda) method [10]. Crystalline phases were observed by an X-ray powder diffractometer (Rigaku, RAD-1VC) at 30 kV and 30 mA with a Cu tube. Crystallite size of platinum was calculated from broadening of a diffraction peak for Pt(111) using the Scherrer's equation. Dispersion of platinum on alumina was measured by a conventional CO chemisorption technique in a helium carrier gas after hydrogen reduction at 400 °C for 15 min. Photographs of platinum particles were taken using a JEOL 2010 transmission electron microscope (TEM) operated at an accelerating voltage of 200 kV.

The oxidation of CO on a catalyst (15 mg) was performed under the gas stream (50 mL min^{-1}) of CO (1 %), O_2 (1 %), and He (98 %); temperature of the catalyst was increased at a constant rate of 10 °C min^{-1}. The reactants (CO and O_2) and product (CO_2) were continuously monitored by a quadrupole mass spectrometer (Anelva, M-200GA-DM).

3 Results

Table 1 shows BET surface area, pore volume and mean pore radius of the cryogels. The surface area decreased with increasing HNO_3/ASB ratio from 158 to 142 $m^2\ g^{-1}$. The surface area decreased with an increase in H_2O/ASB ratio in the range of 29–68 whereas it increased with the ratio in the range of 68–126, giving a minimum value of 135 $m^2\ g^{-1}$ at the ratio of 68. The pore volume showed similar tendency to that of the surface area; the volume decreased with HNO_3/ASB ratio from 0.34 to 0.24 $cm^3\ g^{-1}$. The volume decreased with H_2O/ASB ratio in the range of 29–87 whereas it increased with the ratio in the range of 87–126, giving a minimum value of 0.25 $cm^3\ g^{-1}$ at 87. Furthermore the tendency of mean pore radius also resembled that of the surface area and pore volume. The pore radius was smaller for higher HNO_3/ASB ratio although the difference was unseen within the range of the ratios of 0.24–0.45. The radius decreased with H_2O/ASB ratio in the range of 29–68 whereas it increased with the ratio in the range of 87–126, giving a minimum value of 2.4 nm at the ratios of 68 and 87.

The BJH analysis showed that a peak was observed at smaller pore radius for higher HNO_3/ASB ratio (Fig. 1), although the difference was very little within the range of the ratios of 0.24–0.45. The peak shifted to small pore radius with an increase in H_2O/ASB ratio in the range of 29–68, whereas it shifted to large pore radius with the ratio in the range of 68–126.

The XRD patterns of the cryogels are shown in Fig. 2. For all the cryogels, a diffraction peak corresponding to Pt^0 (111) was seen at $2\theta = 39.7$ degrees in addition to the diffraction peaks for γ-Al_2O_3. The crystallite size of platinum was calculated from the peak broadening and summarized in Table 1. A smaller value of 24 nm was obtained at HNO_3/ASB ratio of 0.24 among runs 1–4. The size decreased with an increase in H_2O/ASB ratio in the range of 29–87, whereas increased with the ratio in the range of 87–126, giving a minimum value of 17 nm at the ratio of 87.

The dispersion of platinum on alumina was calculated from CO adsorption and summarized in Table 1. Very little dispersions were obtained for all the cryogels; among them however run 8 showed relatively high dispersion above 4 %. Because of the difficulty in understanding the tendency of dispersion under the severe heat-resistant conditions, the dispersion was obtained also after heating at 800 °C for 2 h (Table 1). The dispersion appeared roughly decreasing with HNO_3/ASB ratio. On the other hand, the dispersion increased with increasing H_2O/ASB ratio in the range of 29–87, whereas it decreased with the ratio in the range of 87–126, giving a maximum value of 17 % at the ratio of 87.

The results of catalytic CO oxidation are shown in Fig. 3. Among runs 1–4, the activity was higher for run 2 (HNO_3/ASB = 0.24), followed by runs 1 (0.14), 3 (0.35), and 4 (0.45). On the other hand, the activity increased with

Table 1 BET surface area, pore volume, mean pore radius, Pt crystallite size, and Pt dispersion of 1 wt% Pt/Al_2O_3 cryogels after heating at 800 °C for 5 h

Run	HNO_3/ASB (mol/mol)	H_2O/ASB (mol/mol)	BET surafce area ($m^2\ g^{-1}$)	Pore volume ($cm^3\ g^{-1}$)	Mean pore radius (nm)	Pt crystallite size (nm)	Pt dispersion (%)	Pt dispersion (800 °C, 2 h) (%)
1	0.14	70	158	0.34	3.5	36	1.2	17
2	0.24	70	149	0.33	2.4	24	0.0	15
3	0.35	70	152	0.30	2.4	39	0.0	4
4	0.45	70	142	0.24	2.4	43	1.1	9
5	0.17	29	177	0.42	4.0	39	1.6	2
6	0.17	49	167	0.35	3.5	36	3.3	10
7	0.17	68	135	0.27	2.4	24	1.3	10
8	0.17	87	147	0.25	2.4	17	4.4	17
9	0.17	107	156	0.32	3.5	34	0.0	12
10	0.17	126	152	0.30	3.5	33	0.0	8

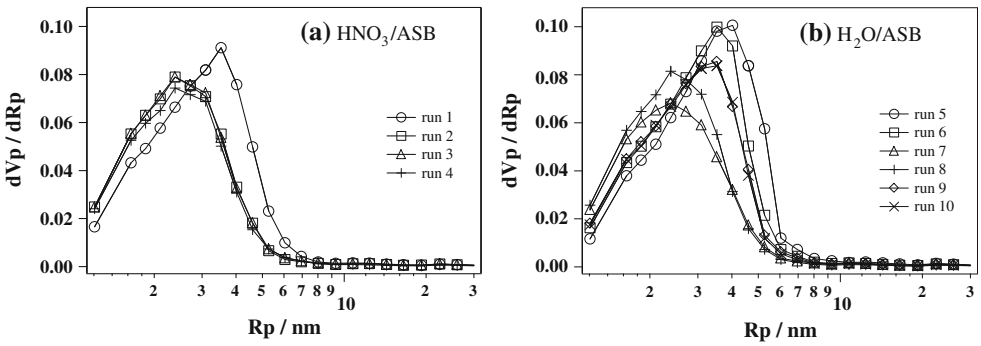

Fig. 1 BJH curves of 1 wt% Pt/Al_2O_3 cryogels after heating at 800 °C for 5 h; effects of **a** HNO_3/ASB and **b** H_2O/ASB ratios

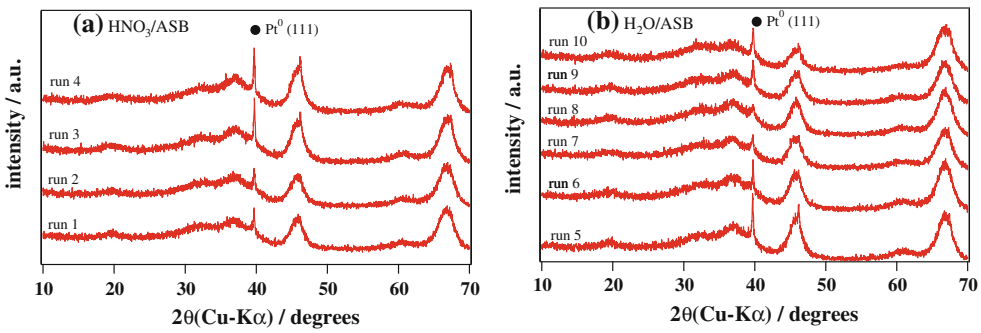

Fig. 2 XRD patterns of 1 wt% Pt/Al_2O_3 cryogels after heating at 800 °C for 5 h; effects of **a** HNO_3/ASB and **b** H_2O/ASB ratios

H_2O/ASB ratio in the range of 29–87, whereas it decreased with the ratio in the range of 87–126, indicating the best ratio of 87 (run 8). The activity of the optimized cryogel was compared to that of the impregnation catalyst in Fig. 4. The activity was higher on the cryogel than on the impregnation catalyst.

XRD patterns of the optimized cryogel and impregnation catalyst are shown in Fig. 5. While the diffraction peaks for Pt^0 were not observed for both catalysts after heating at 500 °C for 1 h, the strong diffraction peaks were seen for the impregnation catalyst after heating at 800 °C for 5 h.

TEM images of platinum on the optimized cryogel and impregnation catalyst are shown in Fig. 6. On the impregnation catalyst sintered platinum particles with sizes more than 100 nm were observed, whereas on the cryogel fine platinum particles with ca. 3–5 nm diameters were also still seen in addition to sintered ones.

4 Discussions

The effect of water content on the structural and textural properties of pure alumina aerogels and xerogels was

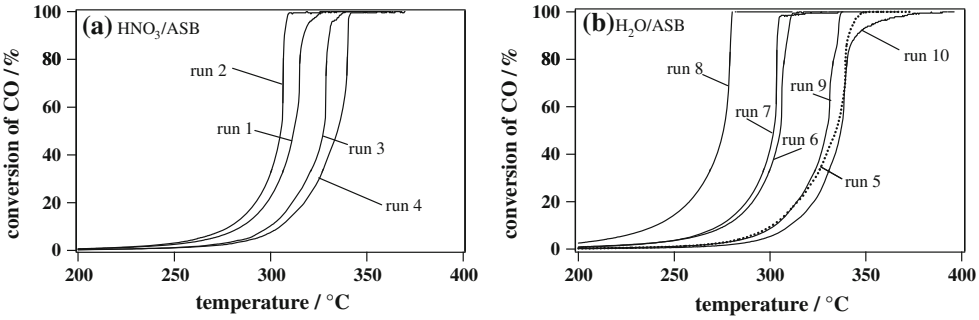

Fig. 3 Catalytic CO oxidation on 1 wt% Pt/Al_2O_3 cryogels after heating at 800 °C for 5 h followed by reduction with hydrogen at 400 °C for 15 min; effects of **a** HNO_3/ASB and **b** H_2O/ASB ratios

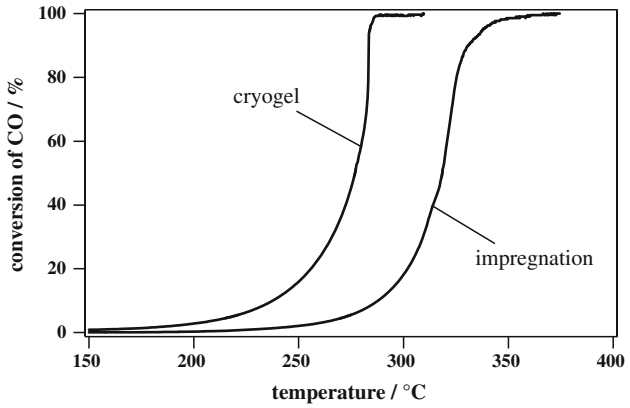

Fig. 4 Catalytic CO oxidation on 1 wt% Pt/Al_2O_3 catalysts after heating at 800 °C for 5 h and subsequent hydrogen reduction at 400 °C for 15 min; cryogel was prepared under the molar ratio of $ASB:HNO_3:H_2O = 1:0.17:87$

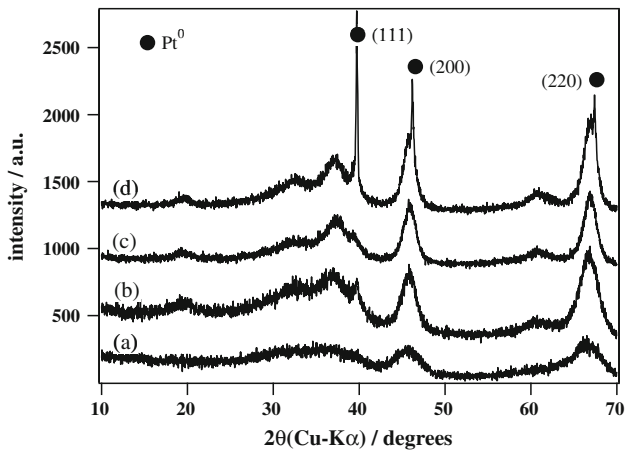

Fig. 5 XRD patterns of 1 wt% Pt/Al_2O_3 catalysts after heating at 500 °C for 1 h and at 800 °C for 5 h *a* cryogel (500 °C) *b* cryogel (800 °C) *c* impregnation catalyst (500 °C), and *d* impregnation catalyst (800 °C). The cryogel was prepared under the molar ratio of $ASB:HNO_3:H_2O = 1:0.17:87$

examined for the sol–gel reactions in alcohols under H_2O/ASB ratios of 1.5–15 [4, 5]. The surface area and pore volume became larger at the stoichiometric ratio of H_2O/ASB = 3. Above this ratio the surface area and pore volume decreased with the ratio whereas the crystallinity of alumina increased. Also for the sol–gel reaction of titanium alkoxide in alcohol to prepare pure titania aerogels, the effects of water and nitric acid contents on the surface area were investigated. The surface area was larger for the stoichiometric ratio of water/titanium n-butoxide = 4, and for nitric acid/titanium n-butoxide ratios of 0.075–0.145 [6]; too high an acid content or too low a hydrolysis level produced soft gels, whereas vice versa the colloidal characteristics prevailed. Different from the sol–gel reactions in alcohols as described above, present one-pot sol–gel processing was carried out by a colloidal method using an aqueous boehmite sol with water/ASB ratios of 29–126 and nitric acid/ASB ratios of 0.14–0.45. Variation of surface area, pore volume, and pore size of the cryogels by varying the ratios of H_2O/ASB and HNO_3/ASB might be ascribed to the differences of length, diameter, degree of intertwining, and/or crystallinity of alumina nanofibers, which may be affected by the rates of hydrolysis, condensation, surface ionization, peptization, and/or gelation [8, 11]. Platinum ions contained in the sol might also affect fine structures and textures of the alumina cryogels. Further studies are still necessary for unambiguous discussions.

It was found, from catalytic CO oxidation, that amount of nitric acid seemed preferable around HNO_3/ASB ratio of 0.24 to achieve the high activity. It was also revealed, from CO chemisorption and XRD analysis, that higher thermal stability was obtained around the HNO_3/ASB ratios of 0.14–0.24. On receiving these results, the examinations of effect of H_2O/ASB ratio on the activity and stability was performed with keeping HNO_3/ASB ratio of 0.17 (runs 5–10). It was revealed that H_2O/ASB ratio was suitable around 87, at the ratio of which more superior CO oxidation activity was observed. In our previous papers one-pot sol–gel reaction was carried out under the conditions of HNO_3/ASB = ca. 0.14 and H_2O/ASB = ca. 47 [2, 3], the ratios of which were close to those for run 6. It can therefore be considered that marked improvement of catalytic activity was attained by optimizing the molar ratio of ASB, nitric acid, and water. The measurements of XRD and CO chemisorption revealed that crystallite size and particle size of platinum became small at H_2O/ASB ratio of 87, which indicates that sintering of platinum was

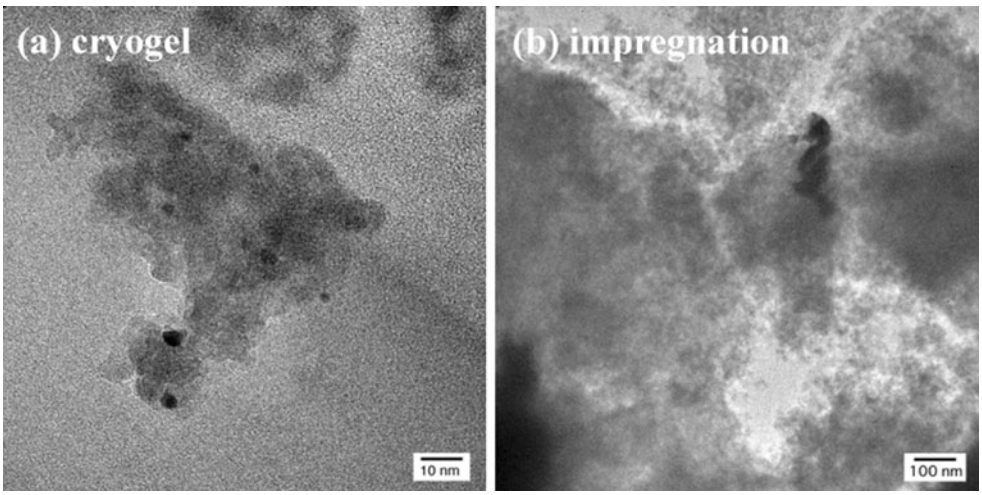

Fig. 6 TEM images of 1 wt% Pt/Al_2O_3 catalysts after heating at 800 °C for 5 h followed by reduction with hydrogen at 400 °C for 15 min **a** cryogel prepared under $ASB:HNO_3:H_2O = 1:0.17:87$, and **b** impregnation catalyst

markedly suppressed at this ratio. The higher oxidation activity at this ratio should be ascribed to the smaller sizes of platinum particles. It was also found, from N_2 adsorption, that surface area, pore volume, and mean pore radius of the cryogel became smaller around this ratio. The results might indicate that platinum was stabilized more markedly in the smaller pores generated by intertwining of alumina nanofibers [9].

It was reported that the sintering of precious metals was retarded when particle size of precious metal was close to pore size of catalyst support [12, 13]. The pores may play a role in trapping the particles and slowing down the rates of their transfer and aggregation. In the optimized cryogel, fine platinum particles with ca. 3–5 nm diameters were still present even after the 800 °C heating as observed by TEM, whereas mean pore diameter was ca. 4.8 nm as obtained by N_2 adsorption. The agreement between the sizes of particles and pores suggests that such nanoparticles were incorporated into the nanopores and stabilized, resulting in the superior CO oxidation activity.

The CO chemisorption showed that Pt dispersion was 38 and 94 % for the optimized cryogel and impregnation catalyst, respectively, after heating at 500 °C for 1 h, whereas 4.4 % and 0.8 %, respectively, after heating at 800 °C for 5 h. The XRD analysis also showed that, while a diffraction peaks for Pt^0 were not observed for both catalysts after the 500 °C heating (Fig. 5) the crystallite size after the 800 °C heating was 17 and 45 nm for the cryogel and impregnation catalyst, respectively. With the impregnation catalyst, most of platinum ions may predominantly be present on the surface of alumina after the impregnation and thereby, the high dispersion as close as 100 % be obtained after the 500 °C heating. With the cryogel, on the other hand, platinum ions may be encapsulated in alumina gel by one-pot sol–gel processing. Such situations should be maintained after the subsequent freeze drying, which should be a principal cause for the lower dispersion after the 500 °C heating. Owing to the encapsulation, however, the sintering of platinum was successfully suppressed at high temperatures, resulting in the higher dispersion after the 800 °C heating. The higher CO oxidation activity on the cryogel was therefore attributable to the smaller sizes of platinum particles remained in the cryogel even after the high temperature heating.

5 Conclusions

By optimizing molar ratio of aluminum alkoxide, nitric acid and water used in one-pot sol–gel reaction for preparing platinum–alumina co-gel, preferable fine structures of the cryogel improving platinum stability and catalytic oxidation activity were obtained. It was found that $ASB:HNO_3:H_2O$ ratio of 1:0.17:87 was better than others to improve the activity and stability, at the ratio of which pore size became smaller. The cryogels may successfully be applicable as high-performance catalysts for automobile emission control where superior thermal stability is required.

Acknowledgments This work has been supported by New Energy and Industrial Technology Development Organization (NEDO) under the sponsorship of Ministry of Economy, Trade and Industry (METI) of Japan.

References

1. The Rare Metal News No. 2506, 24th October, 2011. ARUMU, Tokyo, p 5
2. Osaki T, Nagashima K, Watari K, Tajiri K (2007) Catal Lett 119:134

3. Osaki T, Nagashima K, Watari K, Tajiri K (2008) J Ceram Soc Jpn 116:505
4. Teichner SJ, Nicolaon GA, Vicarini MA, Gardes GEE (1976) Adv Colloid Interface Sci 5:245
5. Balakrishnan K, Gonzalez RD (1993) J Catal 144:395
6. Campbell LK, Na BK, Ko EI (1992) Chem Mat 4:1329
7. Dagan G, Tomkiewicz M (1993) J Phys Chem 97:12651
8. Dagan G, Tomkiewicz M (1994) J Non-Cryst Solids 175:294
9. Osaki T, Yamada K, Watari K, Tajiri K, Shima S, Miki T, Tai Y (2012) J Sol–Gel Sci Tech 61:268
10. Barrett EP, Joyner LG, Halenda PH (1951) J Am Chem Soc 73:373
11. Lofftus KD, Sastry KVS, Hunt AJ (1990) In: Advanced materials proceedings 90, Chap. 26. SME, Littleton
12. Zou WQ, Gonzalez RD (1993) Appl Catal A 102:181
13. Ruckenstein E (1975) J Catal 37:416